

Received September 1, 2019, accepted October 3, 2019, date of publication October 11, 2019, date of current version October 23, 2019.

Digital Object Identifier 10.1109/ACCESS.2019.2946615

# ML-Type EM-Based Estimation of Fast Time-Varying Frequency-Selective Channels Over SIMO OFDM Transmissions

SOUHEIB BEN AMOR<sup>1</sup>, SOFIÈNE AFFES<sup>1</sup>, (Senior Member, IEEE), FAOUZI BELLILI<sup>2</sup>, AND DUSH NALIN JAYAKODY<sup>3,4</sup>, (Senior Member, IEEE)

<sup>1</sup>INRS-EMT, Université du Québec, Montréal, QC H5A 1K6, Canada

<sup>2</sup>Department of Electrical and Computer Engineering, University of Manitoba, Winnipeg, MB R3T 2N2, Canada

<sup>3</sup>School of Computer Science and Robotics, National Research Tomsk Polytechnic University, 634050 Tomsk, Russia

<sup>4</sup>Faculty of Engineering, Sri Lanka Technological Campus, Padukka, Sri Lanka

Corresponding author: Souheib Ben Amor (souheib.ben.amor@emt.inrs.ca)

This work was supported in part by the Discovery Grants (DG) and CREATE PERSWADE <www.create-perswade.ca> Programs of NSERC, and in part by the Discovery Accelerator Supplement Award from NSERC.

**ABSTRACT** This paper investigates the problem of fast time-varying frequency-selective (i.e., multipath) channel estimation over single-input multiple-output orthogonal frequency-division multiplexing (SIMO OFDM)-type transmissions. We do so by tracking the variations of each complex gain coefficient using a polynomial-in-time expansion. To that end, we derive the log-likelihood function (LLF) both in the data-aided (DA) and non-data-aided (NDA) cases. The DA maximum likelihood (ML) estimates over fast SIMO OFDM channels are derived here for the first time in closed-form expressions and hereby shown to be limited to applying over each receive antenna the DA least squares (LS) estimator tailored in [1] to fast SISO OFDM channels. This DA ML is used to initialize periodically, over a relatively large number of data blocks (i.e., with further reduced and relatively close-to-negligible pilot overhead compared to DA ML), a new expectation maximization (EM) ML-type solution we developed here in the NDA case to iteratively maximize the LLF. We also introduce an alternative regularized DA ML (RDM) initialization solution no longer requesting - in contrast to DA ML - more per-carrier pilot frames than the number of paths to further reduce overhead without incurring significant performance losses. Simulation results show that the proposed hybrid ML-EM estimator (i.e., combines all new NDA ML-EM and DA ML or RDM versions) converges within few iterations, thereby providing very accurate estimates of all multipath channel gains. Most importantly, this increased estimation accuracy translates into very significant BER and link-level per-carrier throughput gains over the best representative benchmark solution available so far for the problem at hand, the SISO DA LS technique in [1] with its new generalization here to SIMO systems.

**INDEX TERMS** Channel estimation, time-varying channel (TVC), OFDM, multi-carrier, single-input multiple-output (SIMO), single-input single-output (SISO), maximum likelihood (ML), expectation maximization (EM), least squares (LS), DA (data-aided), NDA (non-data-aided), regularized DA ML (RDM), maximum a posteriori (MAP), inter-carrier interference (ICI) cancellation (ICIC).

## I. INTRODUCTION

Orthogonal frequency-division multiplexing (OFDM) showed its effectiveness in current 4<sup>th</sup> generation wireless technology (4G). A scalable variety of CP-OFDM is already included in 5<sup>th</sup> generation (5G) new radio (NR) standards by the 3<sup>rd</sup> Generation Partnership Project (3GPP) [2]. The adopted waveform will include multiple sub-carrier spacings that depend on the type of deployments and service

The associate editor coordinating the review of this manuscript and approving it for publication was Zilong Liu<sup>1</sup>.

requirements. Moreover, when coupled with the large-scale antenna technology OFDM is poised to enable the 1000-fold increase in capacity that is required over the next few years. Despite its attractive features such as robustness to frequency selective channels and spatial diversity, OFDM-type radio interface technologies (RITs) are already very sensitive to channel time variations since the latter break the crucial orthogonality between the subcarriers thereby introducing the so-called inter-carrier interference (ICI). Accurate channel estimation, hence, becomes a daunting task at very high mobility [3].

So far, a number of channel estimation techniques have been reported in the literature. They can be categorized in two major categories: *i*) the data-aided (DA) approaches where the transmitted symbols are assumed to be perfectly known at the receiver. They provide highly-accurate channel estimates performance at a significant cost, however, in terms of overhead; *ii*) the blind or non-data-aided (NDA) approaches where the receiver has no *a priori* information about the transmitted data. Therefore, NDA techniques do not incur any overhead at the cost, however, of reduced accuracy. Some NDA parameter estimation approaches available in the literature (mainly proposed by the authors' group e.g., see [4]–[7]) occasionally or intermittently operate an initialization step at much less frequent pilot insertion instants (by an order or two of magnitude). Referred to as hybrid (i.e., combine NDA and DA), these techniques very often perform much better than full NDA approaches (i.e., with random initialization). While at the same time they require negligible overhead amounts compared to DA solutions [5]. Hence, we shall advocate a hybrid approach in this work.

For fast time-varying channels, most of the DA techniques rely on a basis expansion model (BEM) to estimate the equivalent discrete-time channel taps [8]–[10]. In fact, BEM methods such as Karhunen-Loeve BEM were designed with low mean square error (MSE) [8]. They are, however, sensitive to statistical channel mismatch. The complex-exponential BEM, also proposed in [8], does not make use of the channel statistics but suffers from large modeling errors. The polynomial BEM (P-BEM) investigated in [9] yields accurate channel estimates, but only at low Dopplers. In [1], the complex gain variations of each path was approximated by a polynomial function of time then estimated by least squares (LS) technique. This solution offers accurate performance even at high Doppler. However, it requires that the number of paths to be smaller than the inserted pilot symbols in each OFDM time slot. Moreover, it was derived in the single-input single-output (SISO) case and its extension to single-input multiple-output (SIMO) systems has never been addressed.

Under the NDA category, time-varying channel estimation was also investigated in [11]. The authors used the discrete Legendre polynomial BEM along with the space alternating generalized expectation maximization (EM)-maximum a posteriori probability (SAGE-MAP) technique to estimate the time-domain channel coefficients of OFDM channels. In [12], we used EM to estimate the channel gains over a SISO configuration. However, both techniques have been tailored for multi-carrier SISO systems and, hence, do not exploit the potential diversity gain achievable by multi-antenna systems. Moreover, they require the number of pilots to be greater than the number of channel paths. In [13], the instantaneous SNR estimation problem was investigated using the EM approach, yet still over SISO configurations only. In [14] and [15], both the EM and LS techniques were again leveraged, respectively, to estimate the SNR over single-carrier SIMO systems. In [16], [17], iterative channel estimation with Kalman filtering and QR detection was first investigated under SISO

multi-carrier channels and later generalized to multiple-input multiple-output (MIMO) OFDM systems. Its performance was further enhanced in [18] by exploiting the statistics of the channel estimation errors in an iterative estimation process. However, Kalman filter-based techniques require perfect knowledge of the Doppler as well as the power-delay profile. Moreover, a high number of pilots per OFDM block is needed to obtain accurate estimates thereby affecting the overall throughput of the system.

In this paper, we develop an iterative EM-based maximum likelihood (ML) estimator of fast time-varying channels over SIMO OFDM-type radio interfaces. By relying on the polynomial approximation of the multipath channel gains [1] and resorting to the powerful EM technique [19] instead of the LS approach, our solution offers a more accurate ML-type acquisition of the polynomial expansion coefficients and the resulting time-varying channel gains. To avoid local convergence that is inherent to iterative algorithms, we initialize the EM algorithm with a SIMO DA ML version developed in this work for that sole purpose. We show that the latter boils down to applying SISO DA LS in [1] over each receive antenna. Besides, coming back to our key contribution here, our new SIMO NDA ML-EM solution, it yields as a byproduct MAP-based soft estimates of the unknown symbols. The latter are leveraged to devise a dedicated ICI cancellation (ICIC) scheme that works side by side with the EM-based time-varying estimator according to the turbo principle (e.g., see [20]). Furthermore, we introduce an alternative SIMO regularized DA ML (RDM) initialization procedure that can still apply when the number of paths exceeds the number of available pilot observations. This desirable feature renders the proposed solution robust to any rapid variations in the propagation environment where the number of paths can change unpredictably due the motion of mobile users. Hence we investigate the possibility of reducing the number of pilots in each OFDM block down below the number of channel paths without significantly affecting the performance. By doing so, we are able to reduce the overhead and eventually increase the throughput quite significantly.

The rest of the paper is organized as follows: In Section II, we introduce the system model. In Section III, we derive a new NDA EM-based ML solution for the underlying estimation problem. In Section IV, we develop a new DA ML version of this estimator over fast SIMO OFDM channels and demonstrate that it amounts to applying the SISO DA LS estimator in [1] separately over each receive antenna. The latter is only run for the initialization of our NDA ML-EM solution at relatively rare pilot insertion instants, resulting in the ultimately proposed new hybrid ML-EM estimator of fast time-varying OFDM channels. In Section V, we use exhaustive computer simulations to assess and confirm the superior performance of the proposed channel estimator not only in terms of component-level channel identification accuracy, but also in terms of much more compelling yet rarely adopted link-level throughput. Finally, we draw out some concluding remarks in Section VI.

The notations adopted in this paper are as follows. Vectors and matrices are represented in lower- and upper-case bold fonts, respectively. Moreover,  $\{\cdot\}^T$  and  $\{\cdot\}^H$  denote the conjugate and Hermitian (i.e., transpose conjugate) operators. The Euclidean norm of any vector is denoted as  $\|\cdot\|$ . For any matrix  $\mathbf{X}$ ,  $[\mathbf{X}]_q$  and  $[\mathbf{X}]_{l,k}$  denote its  $q^{\text{th}}$  column and  $(l, k)^{\text{th}}$  entry, respectively. For any vector  $\mathbf{x}$ ,  $\text{diag}\{\mathbf{x}\}$  refers to the diagonal matrix whose elements are those of  $\mathbf{x}$ . Moreover,  $\{\cdot\}^*$ ,  $\angle\{\cdot\}$ , and  $|\cdot|$  return the conjugate, angle, and modulus of any complex number, respectively. Finally,  $\mathbb{E}\{\cdot\}$  stands for the statistical expectation,  $j$  is the pure imaginary number (i.e.,  $j^2 = -1$ ), and the notation  $\triangleq$  is used for definitions.

## II. SYSTEM MODEL

Consider a SIMO OFDM system with  $N_r$  receiving antenna elements,  $N$  subcarriers, and a cyclic prefix (CP) of a length  $N_{cp}$ . The wireless link between the transmitter and the  $\{r^{\text{th}}\}_{r=1}^{N_r}$  antennas is modeled as a multipath fading channel as follows:

$$h_r(t, \tau) = \sum_{l=1}^{L_r} \alpha_{l,r}(t) \delta(\tau - \tau_{l,r} T_s), \quad (1)$$

where  $L_r$  is the number of paths of the  $r^{\text{th}}$  wireless link. For each path, the delay  $\tau_{l,r}$  is normalized by the sampling period  $T_s$  and the complex gain  $\alpha_{l,r}(t)$  is modeled by a Rayleigh random variable with zero mean and a variance  $\sigma_{l,r}^2$ . The multipath power profile (i.e., the channel) is assumed to be normalized (i.e.,  $\sum_{l=1}^{L_r} \sigma_{l,r}^2 = 1$ ). For each of the  $N_r$  links, we approximate the sampled complex gain of the  $l^{\text{th}}$  path within the duration of  $N_c$  consecutive OFDM blocks,  $\alpha_{l,r} = [\alpha_{l,r}(-N_{cp} T_s), \dots, \alpha_{l,r}(N_b N_c - N_{cp} - 1)]^T$ , by a polynomial of order  $N_c - 1$  as follows [1]:

$$\alpha_{l,r}(p T_s) \approx \sum_{d=1}^{N_c} c_{d,l,r} p^{(d-1)} + \zeta_{l,r}[p], \quad (2)$$

where  $p \in [-N_{cp}, -N_{cp} + 1, \dots, N_b N_c - N_{cp} - 1]$ . Moreover,  $\mathbf{c}_{l,r} = [c_{1,l,r}, c_{2,l,r}, \dots, c_{N_c,l,r}]^T$  gathers the approximating polynomial coefficients corresponding to the  $l^{\text{th}}$  path between the transmitter and the  $r^{\text{th}}$  receiving antenna while  $\zeta_{l,r}[p]$  is the approximation error.  $T = N_b T_s$  denotes the OFDM block duration where  $N_b = N + N_{cp}$ . At the destination, after removing the CP and applying a  $N$ -point fast Fourier transform (FFT), the collected OFDM symbols at each local approximation window of  $N_c$  OFDM blocks (i.e.,  $k = 1, 2, \dots, N_c$ ), over the  $r^{\text{th}}$  antenna element, can be written as follows:

$$\tilde{\mathbf{y}}_{k,r} = \mathbf{H}_{k,r} \mathbf{a}_k + \mathbf{w}_{k,r}, \quad (3)$$

where  $\tilde{\mathbf{y}}_{k,r} = [y_{k,r}[1], y_{k,r}[2], \dots, y_{k,r}[N]]^T$  is the received  $k^{\text{th}}$  OFDM block, and  $\mathbf{w}_{k,r} = [w_{k,r}[1], w_{k,r}[2], \dots, w_{k,r}[N]]^T$  is the complex white Gaussian noise vector with covariance  $\sigma^2 \mathbf{I}_N$  where  $\mathbf{I}_N$  is the  $N$ -dimensional identity matrix. The  $N$  transmitted symbols during the  $k^{\text{th}}$  OFDM block,  $\mathbf{a}_k = [a_k[1], a_k[2], \dots, a_k[N]]^T$ , are generated randomly

from a  $M$ -ary constellation alphabet, denoted  $\mathcal{C}^M$ , and are assumed equally likely, i.e.,  $\{P_r(a_m) = \frac{1}{M}\}_{a_m \in \mathcal{C}^M}$ . The  $N \times N$  matrix,  $\mathbf{H}_{k,r}$ , is the channel frequency response whose elements are given by:

$$[\mathbf{H}_{k,r}]_{m,n} = \frac{1}{N} \sum_{l=1}^{L_r} \left[ e^{-j2\pi \left( \frac{n-1}{N} - \frac{1}{2} \right) \tau_{l,r}} \sum_{q=0}^{N-1} \alpha_{k,l,r}(q T_s) e^{j2\pi \frac{n-m}{N} q} \right], \quad (4)$$

where  $\{\alpha_{k,l,r}(q T_s)\}_{q=k N_b}^{k N_b + N - 1}$  are the samples corresponding to the  $l^{\text{th}}$  path within the duration of the  $k^{\text{th}}$  OFDM block over the  $r^{\text{th}}$  receiving antenna. As shown in [1], with the above approximation [1], the polynomial coefficients,  $\mathbf{c}_{l,r}$  can be obtained using the time average of the channel gain over the effective duration of each OFDM time slot ( $\{\bar{\alpha}_{k,l,r} = \frac{1}{N} \sum_{q=k N_b}^{k N_b + N - 1} \alpha_{k,l,r}(q T_s)\}_{k=0}^{N_c - 1}$ ) as follows:

$$\mathbf{c}_{l,r} = \mathbf{T}^{-1} \bar{\alpha}_{l,r}, \quad (5)$$

where  $\bar{\alpha}_{l,r} = [\bar{\alpha}_{1,l,r}, \bar{\alpha}_{2,l,r}, \dots, \bar{\alpha}_{N_c,l,r}]^T$  and  $\mathbf{T}$  is a  $(N_c \times N_c)$  matrix given by:

$$\mathbf{T} = \begin{pmatrix} 1 & \frac{N-1}{2} & \frac{(N-1)(2N-1)}{6} \\ 1 & \frac{N-1}{2} + N_b & \frac{(N-1)(2N-1)}{6} + (N-1)N_b + N_b^2 \\ 1 & \frac{N-1}{2} + 2N_b & \frac{(N-1)(2N-1)}{6} + 2(N-1)N_b + 4N_b^2 \end{pmatrix}$$

Using these coefficients, the samples of the complex gain of each channel path over the interval  $[-N_{cp}, \dots, N_b N_c - N_{cp} - 1]$ ,  $\mathbf{c}_l = [c_{1,l,r}, c_{2,l,r}, \dots, c_{N_c,l,r}]$ , can be obtained as follows:

$$\alpha_{l,r} = \mathbf{S}^T \mathbf{c}_{l,r}, \quad (6)$$

where  $\mathbf{S}$  is a  $(N_c \times N_b N_c)$  matrix whose elements are given by:

$$\left\{ \{[\mathbf{S}]_{d,p'} = (p' - N_{cp} - 1)^{d-1}\}_{p'=1}^{N_b N_c} \right\}_{d=1}^{N_c}. \quad (7)$$

The channel gains can be estimated using (6) from the channel coefficient estimates whose estimation in (5) ultimately requires an estimate for the channel gain time averages vector  $\bar{\alpha}_{l,r}$ .

In [1],  $\bar{\alpha}_{l,r}$  is estimated by SISO DA LS over  $N_p$  per-carrier pilot frames inserted in each OFDM block in the case of SISO systems (i.e.,  $N_r = 1$ ). Two more processing blocks of i) iterative ICIC and ii) frequency-domain smoothing (to take advantage of the previous  $N_c - 1$  estimates of  $\{\bar{\alpha}_{k,l,1}\}_{k=0}^{N_c-2}$ ) then follow to improve estimation accuracy and speed up convergence. However, increasing performance requires a relatively large number of pilot symbols per block. Moreover, the LS solution requires the number of per-carrier pilot frames to be greater than the number of paths at each antenna element.

In the following, we address the problem of estimating  $\bar{\alpha}_{l,r}$  in SIMO systems (i.e.,  $N_r \geq 1$ ) using all data symbols available at each OFDM block, not only pilots. By doing

so, we develop a new ML-type EM solution that is able to significantly improve performance while keeping the same overhead or otherwise reducing it. Accuracy can be further enhanced as in [1] by suppressing the ICI components from the received signal.

### III. NEW NDA ML-EM ESTIMATOR

We start by stacking the received samples at the output of all the antenna elements,  $\left\{ \left\{ y_{k,r}(n) \right\}_{n=1}^N \right\}_{k=0}^{N_c-1}$ , into vectors  $\left\{ \mathbf{y}_k(n) = [y_{k,1}(n), y_{k,2}(n), \dots, y_{k,N_r}(n)]^T \right\}_{n=1}^N$ . We also define  $\bar{\boldsymbol{\varphi}}_k = [\bar{\varphi}_{k,1}^T, \bar{\varphi}_{k,2}^T, \dots, \bar{\varphi}_{k,N_r}^T]$  as the vectors containing all the time averages of the channel gains of all  $\{L_r\}_{r=1}^{N_r}$  paths with  $\{\bar{\alpha}_{k,r} = [\bar{\alpha}_{k,r,1}, \bar{\alpha}_{k,r,2}, \dots, \bar{\alpha}_{k,r,L_r}]^T\}_{r=1}^{N_r}$ . The probability density function (pdf) of the received samples  $\{\mathbf{y}_k(n)\}_{n=1}^N$  conditioned on the transmitted symbol  $a_k[n]$  and parametrized by  $\boldsymbol{\psi}_k = [\bar{\boldsymbol{\varphi}}_k^T, \sigma^2]^T$ , is expressed as follows:

$$p(\mathbf{y}_k(n)|a_k[n] = a_m; \boldsymbol{\psi}_k) = \frac{1}{(2\pi\sigma^2)^{N_r}} \exp \left\{ \frac{-1}{2\sigma^2} \sum_{r=1}^{N_r} |y_{k,r}(n) - a_m \mathbf{H}_{k,r} \mathbf{1}_{n,n}|^2 \right\}, \quad (8)$$

where:

$$[\mathbf{H}_{k,r}]_{n,n} = \frac{1}{N} \sum_{l=1}^{L_r} \left[ e^{-j2\pi \left( \frac{n-1}{N} - \frac{1}{2} \right) \tau_{l,r}} \sum_{q=0}^{N-1} \alpha_{l,k,r}(qT_s) \right], \quad (9)$$

Note that, for the time being, we absorb the effect of the ICI in the additive noise and we also assume that normalized delays,  $\{\tau_{l,r}\}_{l=1}^{L_r}$ , are perfectly known to the receiver. The  $n^{th}$  diagonal element of the matrix  $\mathbf{H}_{k,r}$  in (9) can then be written as follows:

$$[\mathbf{H}_{k,r}]_{n,n} = \bar{\boldsymbol{\varphi}}_{k,r}^T \mathbf{F}_{n,r}, \quad (10)$$

where  $\mathbf{F}_{n,r}$  is a vector containing the elements of the  $m^{th}$  row of the  $(N \times L_r)$  matrix  $\mathbf{F}_r$  which is defined as:

$$[\mathbf{F}_r]_{m,l} = e^{-j2\pi \left( \frac{m-1}{N} - \frac{1}{2} \right) \tau_{l,r}}. \quad (11)$$

By injecting (10) back into (8), we obtain the following result:

$$p(\mathbf{y}_k(n)|a_k[n] = a_m; \boldsymbol{\psi}_k) = \frac{1}{(2\pi\sigma^2)^{N_r}} \times \exp \left\{ \frac{-1}{2\sigma^2} \sum_{r=1}^{N_r} \left| y_{k,r}(n) - a_m \bar{\boldsymbol{\varphi}}_{k,r}^T \mathbf{F}_{n,r} \right|^2 \right\}. \quad (12)$$

Now, by averaging (12) over the alphabet, the pdf of the received samples can be written as follows:

$$p(\mathbf{y}_k(n); \boldsymbol{\psi}_k) = \sum_{m=1}^M P_r(a_m) p(\mathbf{y}_k(n)|a_k[n] = a_m; \boldsymbol{\psi}_k). \quad (13)$$

As mentioned earlier, the transmitted symbols are generated from a normalized  $M$ -ary constellation (i.e., PAM, PSK or QAM). It follows that:

$$p(\mathbf{y}_k(n); \boldsymbol{\psi}_k) = \frac{1}{M(2\pi\sigma^2)^{N_r}} \times \sum_{m=1}^M \exp \left\{ -\frac{1}{2\sigma^2} \sum_{r=1}^{N_r} \left| y_{k,r}(n) - a_m \bar{\boldsymbol{\varphi}}_{k,r}^T \mathbf{F}_{n,r} \right|^2 \right\}. \quad (14)$$

It is obvious at this stage that maximizing (14) with respect to  $\boldsymbol{\psi}_k$  is analytically intractable. Thus, we will resort to the EM concept to find the maximum of the multidimensional likelihood function (LF). First, we define the log-LF (LLF),  $\mathcal{L}(\boldsymbol{\psi}_k | a_k[n] = a_m) \triangleq \ln(p(\mathbf{y}_k(n) | a_k[n] = a_m; \boldsymbol{\psi}_k))$ , of  $\mathbf{y}_k(n)$  conditioned on the transmitted symbol  $a_k[n]$  for the  $k^{th}$  OFDM symbol which can be written as:

$$\begin{aligned} \mathcal{L}(\boldsymbol{\psi}_k | a_k[n] = a_m) &= -N_r \ln(2\pi\sigma^2) - \frac{1}{2\sigma^2} \left( \sum_{r=1}^{N_r} |y_{k,r}(n)|^2 + \left| a_m \bar{\boldsymbol{\varphi}}_{k,r}^T \mathbf{F}_{n,r} \right|^2 - 2\Re \left\{ y_{k,r}(n)^* a_m \bar{\boldsymbol{\varphi}}_{k,r}^T \mathbf{F}_{n,r} \right\} \right). \end{aligned} \quad (15)$$

During the ‘‘expect step (E-STEP)’’ of the EM algorithm, we compute the expectation of the LLF in (15) over all possible transmitted symbols,  $\{a_m\}_{m=1}^M$ , using the previous estimates of the underlying unknown parameters. Then, the resulting expectation is maximized with respect to the unknown coefficient  $\boldsymbol{\psi}_k$  during the ‘‘Maximization step (M-STEP)’’. Starting with an initial guess,  $\hat{\boldsymbol{\psi}}_k^{(0)}$ , of the channel estimates, the cost function to be maximized during the M-STEP at the  $i^{th}$  EM iteration is given by:

$$\begin{aligned} \mathcal{Q}(\boldsymbol{\psi}_k | \hat{\boldsymbol{\psi}}_k^{(i-1)}) &= \sum_{n=1}^N E_{a_m} \left\{ \mathcal{L}(\boldsymbol{\psi}_k | a_k[n] = a_m) \middle| \mathbf{y}_k(n); \hat{\boldsymbol{\psi}}_k^{(i-1)} \right\}, \end{aligned} \quad (16)$$

where  $E_{a_m}\{\cdot\}$  denotes the expectation over all possible transmitted symbols  $\{a_m\}_{m=1}^M$  and  $\hat{\boldsymbol{\psi}}_k^{(i-1)} = [\hat{\boldsymbol{\varphi}}_k^{(i-1)T}, \hat{\sigma}_k^{(i-1)2}]^T$  contains the estimates of  $\boldsymbol{\psi}_k$  and the noise variance at the  $(i-1)^{th}$  EM iteration. The expression in (16) can be further simplified as follows:

$$\begin{aligned} \mathcal{Q}(\boldsymbol{\psi}_k | \hat{\boldsymbol{\psi}}_k^{(i-1)}) &= -NN_r \ln(2\pi\sigma^2) - \frac{1}{2\sigma^2} \left( \sum_{r=1}^{N_r} Z_{k,r} + \sum_{n=1}^N \gamma_{n,k}^{(i-1)} \left| \bar{\boldsymbol{\varphi}}_{k,r}^T \mathbf{F}_{n,r} \right|^2 - 2\beta_{n,k,r}^{(i-1)} \right), \end{aligned} \quad (17)$$

where<sup>1</sup>:

$$Z_{k,r} = \sum_{n=1}^N |y_{k,r}(n)|^2, \quad (18)$$

<sup>1</sup>For the particular case of normalized-energy constant-envelope constellations, note that we have  $\gamma_{n,k}^{(i-1)} = 1$ .

$$\gamma_{n,k}^{(i-1)} = E_{a_m} \left\{ |a_m|^2 |y_k(n); \widehat{\boldsymbol{\psi}}_k^{(i-1)} \right\}, \quad (19)$$

$$\beta_{n,k,r}^{(i-1)} = E_{a_m} \left\{ \Re \left\{ y_{k,r}(n)^* a_m \bar{\boldsymbol{\varphi}}_{k,r}^T \mathbf{F}_{n,r} \right\} | y_k(n); \widehat{\boldsymbol{\psi}}_k^{(i-1)} \right\}. \quad (20)$$

Using the Bayes formula, the a posteriori probability of  $a_m$ ,  $P_{m,n,k}^{(i-1)} = P_r(a_m | y_k(n); \widehat{\boldsymbol{\psi}}_k^{(i-1)})$ , at the  $(i-1)^{th}$  iteration is given by:

$$P_r(a_m | y_k(n); \widehat{\boldsymbol{\psi}}_k^{(i-1)}) = \frac{P_r(a_m) P(y_k(n) | a_m; \widehat{\boldsymbol{\psi}}_k^{(i-1)})}{P(y_k(n); \widehat{\boldsymbol{\psi}}_k^{(i-1)})}. \quad (21)$$

Since the transmitted symbols are equiprobable (i.e.,  $P_r(a_m) = \frac{1}{M}$ ), we have the following result:

$$P(y_k(n); \widehat{\boldsymbol{\psi}}_k^{(i-1)}) = \frac{1}{M} \sum_{n=1}^N P(y_k(n) | a_m; \widehat{\boldsymbol{\psi}}_k^{(i-1)}). \quad (22)$$

Exploiting the fact that  $\bar{\boldsymbol{\varphi}}_{k,r} = \Re\{\bar{\boldsymbol{\varphi}}_{k,r}\} + j\Im\{\bar{\boldsymbol{\varphi}}_{k,r}\}$  and  $\mathbf{F}_{n,r} = \Re\{\mathbf{F}_{n,r}\} + j\Im\{\mathbf{F}_{n,r}\}$ , the cost function in (17) can be written as follows:

$$\begin{aligned} \mathcal{Q}(\boldsymbol{\psi}_k | \widehat{\boldsymbol{\psi}}_k^{(i-1)}) &= -NN_r \ln(2\pi\sigma^2) - \frac{1}{2\sigma^2} \left( \sum_{r=1}^{N_r} Z_{k,r} + \sum_{n=1}^N \gamma_{n,k}^{(i-1)} \right. \\ &\quad \times \left( \mathbf{F}_{n,r}^H \mathbf{G}_{1,k,r} \mathbf{F}_{n,r} + \Im\{\mathbf{F}_{n,r}\}^T \mathbf{G}_{2,k,r} \Re\{\mathbf{F}_{n,r}\} \right. \\ &\quad \left. \left. + \Re\{\mathbf{F}_{n,r}\}^T \mathbf{G}_{3,k,r} \Im\{\mathbf{F}_{n,r}\} \right) \right. \\ &\quad \left. - 2 \sum_{m=1}^M P_{m,n,k}^{(i-1)} \eta_{k,n,r}^{(m)} \right), \quad (23) \end{aligned}$$

where:

$$\begin{aligned} \mathbf{G}_{1,k,r} &= \Re\{\bar{\boldsymbol{\varphi}}_{k,r}\} \Re\{\bar{\boldsymbol{\varphi}}_{k,r}\}^T + \Im\{\bar{\boldsymbol{\varphi}}_{k,r}\} \Im\{\bar{\boldsymbol{\varphi}}_{k,r}\}^T, \\ \mathbf{G}_{2,k,r} &= \Re\{\bar{\boldsymbol{\varphi}}_{k,r}\} \Im\{\bar{\boldsymbol{\varphi}}_{k,r}\}^T - \Im\{\bar{\boldsymbol{\varphi}}_{k,r}\} \Re\{\bar{\boldsymbol{\varphi}}_{k,r}\}^T, \\ \mathbf{G}_{3,k,r} &= \Im\{\bar{\boldsymbol{\varphi}}_{k,r}\} \Re\{\bar{\boldsymbol{\varphi}}_{k,r}\}^T - \Re\{\bar{\boldsymbol{\varphi}}_{k,r}\} \Im\{\bar{\boldsymbol{\varphi}}_{k,r}\}^T, \\ \eta_{k,n,r}^{(m)} &= \Re\{y_{k,r}(n)^* a_m \mathbf{F}_{n,r}^T\} \Re\{\bar{\boldsymbol{\varphi}}_{k,r}\} \\ &\quad - \Im\{y_{k,r}(n)^* a_m \mathbf{F}_{n,r}^T\} \Im\{\bar{\boldsymbol{\varphi}}_{k,r}\}. \quad (24) \end{aligned}$$

As per the M-STEP, we differentiate the cost function in (23) with respect to  $\Re\{\bar{\boldsymbol{\varphi}}_{k,r}\}$  and  $\Im\{\bar{\boldsymbol{\varphi}}_{k,r}\}$  and set the result to zero to obtain the following results:

$$\begin{aligned} \sum_{n=1}^N \gamma_{n,k}^{(i-1)} \left( \mathbf{J}_{1,n,r} \Re\{\bar{\boldsymbol{\varphi}}_{k,r}\} - \mathbf{J}_{2,n,r} \Im\{\bar{\boldsymbol{\varphi}}_{k,r}\} \right) &= \sum_{n=1}^N \boldsymbol{\mu}_{1,n,k,r}, \\ \sum_{n=1}^N \gamma_{n,k}^{(i-1)} \left( \mathbf{J}_{1,n,r} \Im\{\bar{\boldsymbol{\varphi}}_{k,r}\} + \mathbf{J}_{2,n,r} \Re\{\bar{\boldsymbol{\varphi}}_{k,r}\} \right) &= -\sum_{n=1}^N \boldsymbol{\mu}_{2,n,k,r}, \end{aligned}$$

where:

$$\begin{aligned} \mathbf{J}_{1,n,r} &= \Re\{\mathbf{F}_{n,r}\} \Re\{\mathbf{F}_{n,r}\}^T + \Im\{\mathbf{F}_{n,r}\} \Im\{\mathbf{F}_{n,r}\}^T, \\ \mathbf{J}_{2,n,r} &= \Re\{\mathbf{F}_{n,r}\} \Im\{\mathbf{F}_{n,r}\}^T - \Im\{\mathbf{F}_{n,r}\} \Re\{\mathbf{F}_{n,r}\}^T, \\ \boldsymbol{\mu}_{1,n,k,r} &= \sum_{m=1}^M P_{m,n,k}^{(i-1)} \Re\{y_{k,r}(n)^* a_m \mathbf{F}_{n,r}^T\}, \\ \boldsymbol{\mu}_{2,n,k,r} &= \sum_{m=1}^M P_{m,n,k}^{(i-1)} \Im\{y_{k,r}(n)^* a_m \mathbf{F}_{n,r}^T\}. \end{aligned}$$

Now, using the identity  $\bar{\boldsymbol{\varphi}}_{k,r} = \Re\{\bar{\boldsymbol{\varphi}}_{k,r}\} + j\Im\{\bar{\boldsymbol{\varphi}}_{k,r}\}$  leads to:

$$\sum_{n=1}^N (\mathbf{J}_{1,n,r} + j\mathbf{J}_{2,n,r}) \gamma_{n,k}^{(i-1)} \bar{\boldsymbol{\varphi}}_{k,r} = \sum_{n=1}^N \boldsymbol{\mu}_{1,n,r} - j\boldsymbol{\mu}_{2,n,r}. \quad (25)$$

Hence, the  $i^{th}$  EM update for time average of the channel gains at the  $i^{th}$  iteration can be obtained as follows:

$$\begin{aligned} \widehat{\boldsymbol{\varphi}}_{k,r}^{(i)} &= \left( \sum_{n=1}^N \gamma_{n,k}^{(i-1)} (\mathbf{J}_{1,n,r} + j\mathbf{J}_{2,n,r}) \right)^{-1} \\ &\quad \times \sum_{n=1}^N \left( \sum_{m=1}^M P_{m,n,k}^{(i-1)} y_{k,r}^* a_m \mathbf{F}_{n,r}^T \right)^H. \quad (26) \end{aligned}$$

Similarly, by differentiating the cost function in (23) with respect to  $\sigma^2$  and setting the result to zero, we obtain the following update for the noise variance:

$$\widehat{\sigma^2}^{(i)} = \frac{\sum_{r=1}^{N_r} Z_{k,r} + \sum_{n=1}^N \left| \mathbf{F}_{n,r}^T \widehat{\boldsymbol{\varphi}}_{k,r}^{(i-1)} \right|^2 \gamma_{n,k}^{(i-1)} - 2\beta_{n,k,r}^{(i-1)}}{2NN_r}. \quad (28)$$

Finally, after  $\mathcal{I}_{EM}$  iterations of the EM algorithm, the channel estimates, corresponding to  $N_c$  consecutive OFDM symbols over the  $r^{th}$  antenna element, are obtained as follows:

$$\widehat{\boldsymbol{\alpha}}_{l,r} = \mathbf{S}^T \widehat{\mathbf{c}}_{l,r} = \mathbf{S}^T \mathbf{T}^{-1} \widehat{\boldsymbol{\alpha}}_{l,r}^{(\mathcal{I}_{EM})}, \quad (29)$$

where  $\widehat{\boldsymbol{\alpha}}_{l,r}^{(\mathcal{I}_{EM})} = [\widehat{\boldsymbol{\alpha}}_{1,l,r}^{(\mathcal{I}_{EM})}, \widehat{\boldsymbol{\alpha}}_{2,l,r}^{(\mathcal{I}_{EM})}, \dots, \widehat{\boldsymbol{\alpha}}_{N_c,l,r}^{(\mathcal{I}_{EM})}]^T$  is the EM-based ML vector estimate of the complex channel gain time averages of the  $l^{th}$  path over  $N_c$  OFDM data symbols. The channel gain estimates in (29) can be further improved by implementing an iterative ICIC technique. Indeed, the channel and symbol estimates provided by the EM algorithm can be used to reconstruct then remove the ICI components from the received signal and the resulting samples can be re-injected once again as new inputs to the EM algorithm to enhance accuracy. In this way, the entire process can be repeated  $\mathcal{I}_{ICIC}$  iterations until no additional improvements can be achieved. ICIC requires decoding the data symbols to be able to reduce the ICI level. Instead of implementing the successive interference cancellation (SIC) at the output of each antenna element as in [1], we make use of the symbols' posteriors,  $P_{m,n,k}^{(\mathcal{I}_{EM})}$ , already provided by the EM algorithm and decode the data symbols according to the MAP criterion as follows:

$$\widehat{a}_k^{(s)}[n] = \underset{a_m \in \mathcal{C}^M}{\operatorname{argmax}} \left| a_m - \sum_{m'=1}^M P_{m',n,k}^{(\mathcal{I}_{EM})} a_{m'} \right|^2, \quad (30)$$

where  $\widehat{a}_k^{(s)}[n]$  is the detected symbol corresponding to the  $n^{th}$  subcarrier of each  $k^{th}$  OFDM block after  $s$  ICIC iterations. At each  $s^{th}$  ICIC iteration, the detected symbols are used to remove the ICI component from the original received signal so as to provide the EM algorithm with less-ISI-corrupted observations. The later is given by:

$$\widetilde{\mathbf{y}}_{k,r}^{(s+1)} = \widetilde{\mathbf{y}}_{k,r} - (\widehat{\mathbf{H}}_{k,r}^{(s,\mathcal{I}_{EM})} - \operatorname{diag}\{\widehat{\mathbf{h}}_{k,r}^{(d,s,\mathcal{I}_{EM})}\}) \widehat{\mathbf{a}}_k^{(s)}, \quad (31)$$

where  $\hat{\mathbf{h}}_{k,r}^{(s,\mathcal{I}_{EM})}$  is a vector containing the diagonal elements of  $\hat{\mathbf{H}}_{k,r}^{(s,\mathcal{I}_{EM})}$ . The latter is the estimate of channel frequency response at the convergence of the EM technique.

#### IV. PROPOSED HYBRID ML-EM ESTIMATOR

Due to its iterative nature, NDA ML-EM requires an initial starting point. One straightforward solution is to settle on a random initial guess. By doing so, the proposed solution preserves its full NDA characteristic. However, with random initialization, the algorithm's convergence to a local minimum becomes extremely high. Hence, we develop a SIMO DA ML version of this estimator for the sole purpose of providing relatively reliable initial values that ensure global convergence of the NDA ML-EM solution. We will show later in this section that this initialization step can be applied at relatively rare pilot insertion instants, giving rise to the ultimately proposed new hybrid ML-EM estimator of fast time-varying OFDM channels.

##### A. INITIALIZATION WITH NEW DA ML

As mentioned above, NDA ML-EM requires a good initial guess in order to return accurate estimates of the channel gains. An intuitive solution for obtaining those initial values is to use the pilot symbols injected at the subcarrier positions  $\{p_1, p_2, \dots, p_{N_p}\}$  within each OFDM block. In the SIMO system, the received  $N_p$  subcarriers at each OFDM block,  $\mathbf{y}_{k,r}^{(p)} = [y_{k,r}(p_1), y_{k,r}(p_2), \dots, y_{k,r}(p_{N_p})]^T$ , corresponding to the pilot positions (by neglecting the ICI) are given by:

$$\tilde{\mathbf{y}}_{k,r}^{(p)} = \text{diag}\{\mathbf{a}_k^{(p)}\} \mathbf{h}_{k,r}^{(p)} + \mathbf{w}_{k,r}^{(p)}, \quad (32)$$

where  $\mathbf{a}_k^{(p)} = [a_k^{(p)}(1), a_k^{(p)}(2), \dots, a_k^{(p)}(N_p)]^T$  are the transmitted pilots within the  $k^{\text{th}}$  OFDM block. The channel frequency response and noise component corresponding to the pilot indices are given by  $\mathbf{h}_{k,r}^{(p)} = [\mathbf{H}_{k,r}]_{p_1,p_1}, [\mathbf{H}_{k,r}]_{p_2,p_2}, \dots, [\mathbf{H}_{k,r}]_{p_{N_p},p_{N_p}}]^T$  and  $\mathbf{w}_{k,r}^{(p)} = [w_{k,r}(p_1), w_{k,r}(p_2), \dots, w_{k,r}(p_{N_p})]^T$ , respectively. By stacking the received pilot samples at the output of the antenna elements into vectors,  $\{\mathbf{y}_k^{(p)}(p_n) = [y_{k,1}(p_n), y_{k,2}(p_n), \dots, y_{k,N_r}(p_n)]^T\}_{n=1}^{N_p}$ , we rewrite (32) as follows:

$$\mathbf{y}_k^{(p)} = \mathbf{A}_k^{(p)} \mathbf{F}^{(p)} \bar{\boldsymbol{\varphi}}_k + \mathbf{w}_k^{(p)}, \quad (33)$$

where  $\mathbf{w}_k^{(p)} = [\mathbf{w}_{k,1}^{(p)T}, \mathbf{w}_{k,2}^{(p)T}, \dots, \mathbf{w}_{k,N_r}^{(p)T}]^T$  and  $\mathbf{A}_k^{(p)}$  is a diagonal matrix given by:

$$\mathbf{A}_k^{(p)} = \mathbf{I}_{N_r} \otimes \text{diag}\{\mathbf{a}_k^{(p)}\}. \quad (34)$$

The matrix  $\mathbf{F}^{(p)}$  is a  $(N_r N_p \times L)$  block-diagonal matrix ( $L = \sum_{r=1}^{N_r} L_r$ ) defined as follows:

$$\mathbf{F}^{(p)} = \text{blkdiag}\{\mathbf{F}_1^{(p)}, \mathbf{F}_2^{(p)}, \dots, \mathbf{F}_{N_r}^{(p)}\}. \quad (35)$$

in which  $\mathbf{F}_r^{(p)}$  contains the rows of the matrices  $\mathbf{F}_r$  that corresponds to the pilot symbols' indices (i.e.,  $\{[\mathbf{F}_r^{(p)}]_{m,l} =$

$[\mathbf{F}_r]_{p_m,l}\}_{m=1}^{N_p}\}_{l=1}^{L_r}$ ). The pdf in the DA case is given by:

$$\begin{aligned} p(\mathbf{y}_k^{(p)} | \mathbf{a}_k^{(p)}; \boldsymbol{\psi}_k) &= \frac{1}{(2\pi\sigma^2)^{N_r N_p}} \\ &\times \exp\left\{-\frac{1}{2\sigma^2} (\mathbf{y}_k - \mathbf{A}_k^{(p)} \mathbf{F}^{(p)} \bar{\boldsymbol{\varphi}}_k)^H (\mathbf{y}_k - \mathbf{A}_k^{(p)} \mathbf{F}^{(p)} \bar{\boldsymbol{\varphi}}_k)\right\}. \end{aligned} \quad (36)$$

The corresponding LLF is given by:

$$\begin{aligned} \mathcal{L}(\boldsymbol{\psi}_k) &= -N_r N_p \ln(2\pi\sigma^2) \\ &- \frac{1}{2\sigma^2} (\mathbf{y}_k - \mathbf{A}_k^{(p)} \mathbf{F}^{(p)} \bar{\boldsymbol{\varphi}}_k)^H (\mathbf{y}_k - \mathbf{A}_k^{(p)} \mathbf{F}^{(p)} \bar{\boldsymbol{\varphi}}_k). \end{aligned} \quad (37)$$

By differentiating (37) with respect to  $\bar{\boldsymbol{\varphi}}_k$ , we obtain the following initial ML-based DA estimates:

$$\hat{\bar{\boldsymbol{\varphi}}}_k^{(0)} = \left(\mathbf{F}^{(p)H} \mathbf{A}_k^{(p)H} \mathbf{A}_k^{(p)} \mathbf{F}^{(p)}\right)^{-1} \mathbf{F}^{(p)H} \mathbf{A}_k^{(p)H} \mathbf{y}_k. \quad (38)$$

Due to the linearity of the observation model in (32) and the Gaussianity of the noise, the new SIMO DA ML estimator reduces in the SISO case to the DA LS estimator in [1], making the former a generalized extension of the latter to SIMO configurations. More importantly, we reveal that the solution in (38) requires the inversion of a block-diagonal matrix whose computation can therefore be decoupled across the receive antennas by separately inverting the  $N_r$  antenna-specific blocks  $\{\mathbf{F}_r^{(p)H} \text{diag}\{\mathbf{a}_k^{(p)}\} \{\mathbf{a}_k^{(p)}\}^H \mathbf{F}_r^{(p)}\}_{r=1}^{N_r}$ . Hence, we prove that the SIMO DA ML solution actually boils down to applying the SISO DA LS in [1] at the output of each receive antenna. Another point worth mentioning here is that the number of pilots  $N_p$  required to obtain initial estimates has to be larger than the number of paths  $L_r$ . The initial estimate of the noise variance can also be obtained by differentiating (37) with respect to  $\sigma^2$  as follows:

$$\hat{\sigma}^2^{(0)} = \frac{1}{2N_p N_r} \left\| \mathbf{y}_k - \mathbf{A}_k^{(p)} \mathbf{F}^{(p)} \hat{\bar{\boldsymbol{\varphi}}}_k^{(0)} \right\|^2. \quad (39)$$

##### B. REDUCTION OF PILOT SUBCARRIERS

Usually, the solution in (38) requires that  $N_p \geq \max\{L_r\}_{r=1}^{N_r}$  otherwise the system of equations is underdetermined and the matrix  $\mathbf{F}_r^{(p)H} \text{diag}\{\mathbf{a}_k^{(p)}\} \{\mathbf{a}_k^{(p)}\}^H \mathbf{F}_r^{(p)}$  is no longer invertible. In this case, the overall throughput will be strongly dependant on the number of paths  $\max\{L_r\}_{r=1}^{N_r}$ . Now since the ML-EM solution relies on those estimates only to trigger the iteration process, we can settle for less reliable initial estimates by reducing the number of pilots per OFDM blocks. Taking into account the fact that the SIMO DA ML solution in (38) corresponds to an ill-posed problem, we opt for a regularization technique to solve this problem. One attracting solution is the Tikhonov regularization [21] which allows us to obtain the initial estimates as follows:

$$\hat{\bar{\boldsymbol{\varphi}}}_k^{(0)} = \left(\mathbf{F}^{(p)H} \mathbf{A}_k^{(p)H} \mathbf{A}_k^{(p)} \mathbf{F}^{(p)} + \lambda \mathbf{I}_L\right)^{-1} \mathbf{F}^{(p)H} \mathbf{A}_k^{(p)H} \mathbf{y}_k. \quad (40)$$

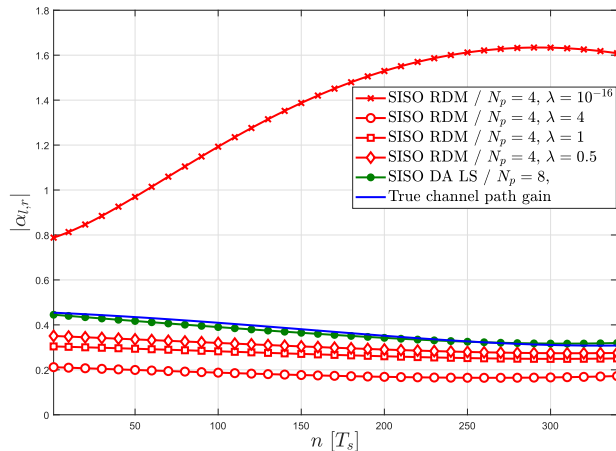


**FIGURE 1.** Channel path gain estimates versus time index over the first  $N_c = 3$  OFDM blocks with the SISO DA LS (8 pilots) and SISO RDM (4 pilots) initialization techniques at  $\text{SNR} = 30$  dB for  $N_r = 1$  and multiple values of  $\lambda$ .

The factor  $\lambda$  is a regularization factor, when set to zero, the solution in (40) becomes equivalent to the one in (38). Mainly, the RDM is developed to improve the conditioning of the problem by adding a regularization factor to the non-invertible matrix,  $\mathbf{F}_r^{(p)H} \text{diag}\{\mathbf{a}_k^{(p)}\}\{\mathbf{a}_k^{(p)}\}^H \mathbf{F}_r^{(p)}$ .

In Fig. 1, we show the effect of the regularization factor on the performance of the RDM estimator. On one hand, if chosen too small (i.e.,  $\lambda = 10e^{-16}$ ), the solution in (40) is close to the original one given in (38). At this point, the RDM may suffer from the same instability issues as the original DA ML solution. On the other hand, if chosen too large (i.e.,  $\lambda = 4$ ), the provided solution will start moving away from the original problem defined in (36). It is worth mentioning that the range of values over which RDM provides acceptable initial values is conveniently large. Hence, an exhaustive search for the optimal regularization factor is not required. Note also that other regularization techniques can be envisioned such as the least absolute shrinkage and selection operator (LASSO) technique [22]. However, the latter, unavailable in a closed-form solution, is usually found using optimization methods such as quadratic programming or convex optimization. Such solution introduces additional computational complexity whereas the Tikhonov regularization keeps the computational burden approximately the same of the original SIMO DA ML.

### C. EXTREME SLOW-UP OF PILOT INSERTION RATE

As mentioned earlier, an initial guess is always required to trigger NDA ML-EM. However, depending on the receiver mobility, the EM technique may use the estimates of the previous OFDM block channel gains as initial candidates for the current one. In the following, we discuss the possibility of reducing the total number of per-carrier pilot frames and, hence, the overhead to achieve higher per-carrier throughput. As depicted in Fig. 2, we show an example of pilots insertion and processing tasks for all possible channel estimation techniques. In the DA case, i.e., Fig.2 (a), the estimation relies on known per-carrier pilot frames at the receiver side.

In this configuration, the DA techniques provide better estimation performance at the expense of significant overhead. Indeed, some subcarriers at each OFDM block are used as pilots for estimation purposes while  $(N - N_p)$  remaining ones carry the useful data. Such approach relies on a trade-off between overhead and estimation performance since the estimation accuracy increases with the number of pilots. In the full NDA case, i.e., Fig.2 (b), the estimation technique uses only the per-carrier data frames to estimate the channel gains. Such technique enjoys zero overhead but suffers from performance degradation especially in high mobility scenarios. With the new hybrid ML-EM, i.e., Fig.2 (c), the initialization technique (SIMO DA ML or its SIMO RDM equivalent at a low number of pilot subcarriers) is performed only once each  $RI$  consecutive  $N_c$  OFDM blocks to trigger the NDA estimation process. Since the channel, even a fast time-varying one, varies relatively slowly with respect to the high sampling or processing rates that characterize new radio access technologies, more so at low and moderate mobilities, there is no need for frequent initialization at each  $N_c$  OFDM blocks. Instead, the EM technique relies on the same estimates provided by NDA ML-EM during the previous  $N_c$  OFDM blocks. In other words, the first  $N_c$  OFDM blocks of a sequence of  $RI$   $N_c$  blocks will be initialized using the DA LS technique. And each of the remaining  $(RI - 1) N_c$  OFDM blocks will be initialized with the channel gain estimates of their predecessors. Thus, the number of inserted pilots can be significantly reduced (by an order or two of magnitude as will be shown later).

Note that the choice of  $RI$ , called hereafter as the refreshment interval, might vary depending on some key parameters. Indeed, from an estimation accuracy point of view,  $RI$  depends mainly on the Doppler frequency and the average per-carrier SNR. From a per-carrier throughput point of view, performance deterioration is expected at higher  $RI$  values in high mobility scenarios. However, such deterioration can have a negligible impact if not any, on decoding performance. Indeed, with the adoption of adaptive modulation, QPSK is adopted at low per-carrier SNR values since it is more robust to estimation errors. At high per-carrier SNR values, the estimation error is less severe and higher modulation orders can be considered since they perform well even with low pilot numbers.

By taking into account all the features mentioned above, the hybrid channel estimation technique can be summarized in Algorithm 1.

Note that the “initialization” condition mentioned in Algorithm 1 controls the rate at which the SIMO RDM is run during the initialization phase.

## V. SIMULATION RESULTS

In this section, we assess the performance of the new EM-based ML time varying channel estimator *i*) at the component level in terms of the mean square error (MSE) of the channel gains (averaged over all antennas), and *ii*) in terms of link-level bit error rate (BER) and per-carrier throughput.

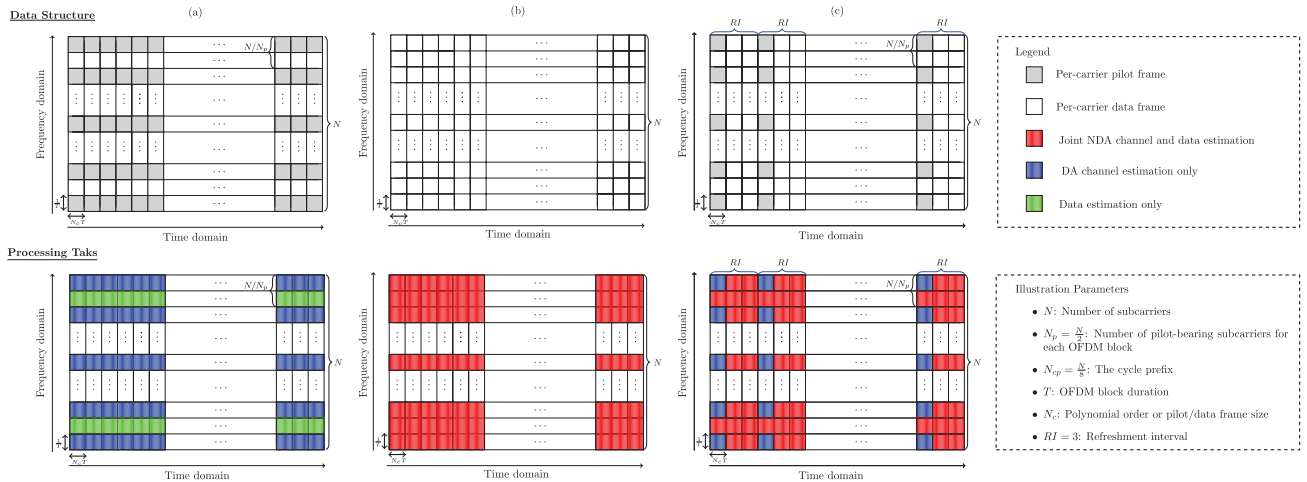


**FIGURE 2.** Data structure and processing tasks for different estimation approaches: (a) SISO DA LS [1] or its proposed SIMO DA ML extension, (b) the new NDA ML-EM, and (c) the advocated new hybrid ML-EM solution (i.e., combines both new NDA ML-EM and DA ML versions).

**Algorithm 1** Joint Hybrid ML-EM Channel and Data Estimation

```

for  $k = 1$  to  $N_c$  do
  if initialization then
    if  $N_p \geq \max\{L_r\}_{r=1}^{N_r}$  then
      Estimate  $\hat{\varphi}_k^{(0)}$  using (38)
    else
      Estimate  $\hat{\varphi}_k^{(0)}$  using (40)
    end if
  else
    Use  $\hat{\varphi}_k^{(k-1)}$  as initial guess
  end if
  Estimate  $\hat{\sigma}^2^{(0)}$  using (39)
end for
while  $s < \mathcal{I}_{ICI}$  do
  for  $k = 1$  to  $N_c$  do
    while  $i < \mathcal{I}_{EM}^{(i)}$  do
      Estimate  $\hat{\varphi}_k^{(i)}$  using (26)
      Estimate the noise variance  $\hat{\sigma}^2^{(i)}$  using (28)
    end while
    Decode the data  $\hat{\mathbf{a}}_k$  using (30)
  end for
  Construct the channel frequency response using  $\{\hat{\alpha}_{l,r}^{(EM)}\}_{l=1}^{L_r}$  as in (4)
  Remove the ICI component using  $\{\hat{\mathbf{a}}_k\}_{k=1}^{N_c}$  as in (31)
end while

```

In all simulations, we consider a SIMO OFDM RIT with  $N = 128$  subcarriers, a cyclic prefix  $N_{cp} = 16$ , and a central frequency  $f_c = 5$  GHz. The sampling period is  $T_s = 0.5 \mu s$ . The channel between the transmitter and each  $r^{th}$  antenna element is modeled by a multipath Rayleigh fading channel where the individual complex path gains,  $\{\alpha_{l,r}(t)\}_{l=1}^{L_r}$ , follow a uniform Jake’s model. We assume, without loss of generality, that the links between the source and the  $N_r$  receiving antennas have the same channel parameters used in [1] listed

**TABLE 1.** Channel parameters.

Path Number	1	2	3	4	5	6
Average Power [dB]	-7.219	-4.219	-6.219	-10.219	-12.219	-14.219
Normalized Delay	0	0.4	1	3.2	4.6	10

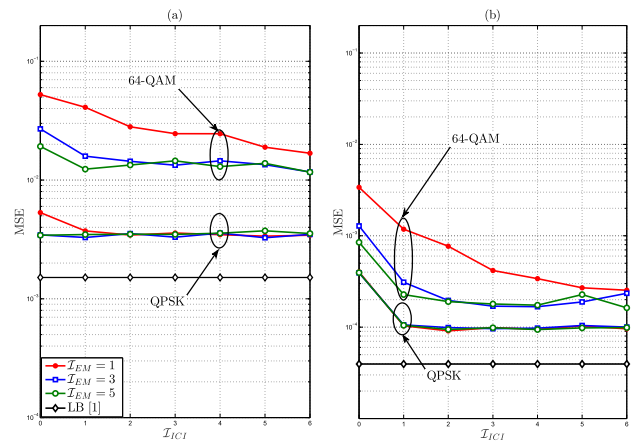


**FIGURE 3.** MSE of the advocated new hybrid ML-EM vs the number of ICIC iterations for QPSK and 64-QAM modulations with  $v = 300$  km/h,  $N_c = 3$ ,  $N_r = 2$ , and  $N_p = 8$  at: (a) SNR = 10 dB, and (b) SNR = 30 dB.

in Table 1. Unless specified otherwise, the initialization step is executed at each OFDM block (i.e.,  $RI = 1$ ).

We start by investigating the effect of the number of EM iterations on the estimation accuracy. To do so, we plot in Fig. 3 the MSE of our proposed estimator (referred to hereafter as hybrid ML-EM) along with the MSE lower bound (LB) derived in [1] against  $R_{EM}$  at two different per-carrier SNR levels and high Doppler (i.e.,  $F_D T = 0.1$ ). The latter translates into a receiver speed of  $v = 300$  km/h ( $v = \frac{F_D v_c}{f_c}$ ,  $v_c$  being the speed of light).

Obviously, at a fixed per-carrier SNR level, the convergence rate of the hybrid ML-EM technique ( $\mathcal{I}_{EM}$ ) is affected by the ICI level corrupting the received samples. In fact, the EM technique is able to converge much faster when the ICI level is reduced with an ICIC technique. For instance, when using QPSK modulation, ML-EM is able to provide the



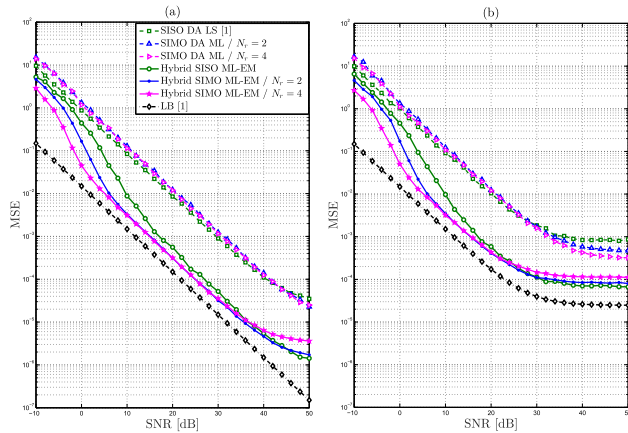


**FIGURE 4.** MSE of the advocated new hybrid ML-EM, the SISO DA LS in [1] (i.e.,  $N_r = 1$ ), and its proposed SIMO DA ML extension vs. the per-carrier SNR for different numbers of receiving antennas with QPSK,  $N_c = 3$  and  $N_p = 8$  at: (a)  $v = 60$  km/h, and (b)  $v = 300$  km/h.

same accuracy either with 1 or 5 EM iterations when ICIC is applied. However, for high modulation order (i.g., 64-QAM) that are usually more sensitive to ICI component, the same technique requires at least 3 EM iterations to converge when ICIC is not implemented.

In Fig. 4, we investigate the influence of the number of receiving antenna elements on the estimation performance. We compare the hybrid ML-EM estimator to the DA LS technique and the LB both derived in [1] in the SISO case and to the generalized DA ML versions proposed here in the SIMO case. We observe a clear advantage of hybrid ML-EM at both low (i.e.,  $F_D T = 0.02$  or equivalently  $v = 60$  km/h) and high (i.e.,  $F_D T = 0.01$  or  $v = 300$  km/h) Dopplers even in the SISO case. As the number of antenna elements increases, hybrid ML-EM exhibits a better estimation accuracy especially at low and medium per-carrier SNR levels. Since hybrid ML-EM takes advantage of the diversity gain of multi-antenna systems, it is able to improve the channel estimates per-antenna. Moreover, the noise variance estimate in (28), provided by hybrid ML-EM is a more accurate as it is averaged over many antenna branches. At high per-carrier SNR, however, we observe that increasing the number of antennas has almost no effect on the estimation accuracy performance. This is due to the noise level being lower than the ICI components. At such per-carrier SNR levels, the channel estimation accuracy is dictated mainly by ICIC capabilities of the proposed design.

In Fig. 5, we evaluate the performance of the proposed technique at low and high mobilities against the DA LS technique and the LB both derived in [1] in the SISO case and to the generalized DA ML versions proposed here in the SIMO case. We observe a clear advantage of the hybrid ML-EM technique at both low and high Dopplers. We also observe that the ICIC block enhances the performance of both techniques. However, hybrid ML-EM benefits from much larger gains and approaches the LB at high per-carrier SNR values. Moreover, we notice that the ICIC block provides enhanced performances only at high per-carrier SNR values.

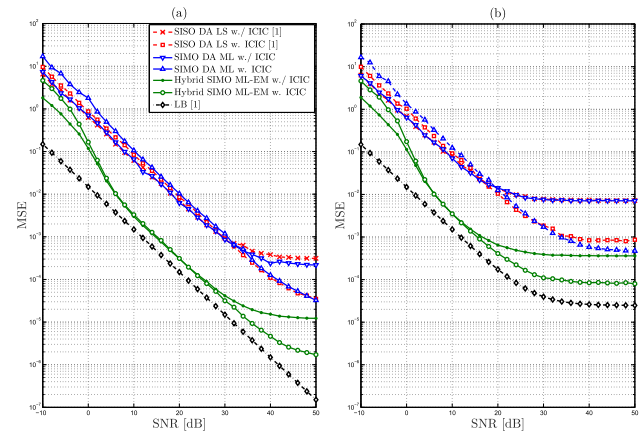


**FIGURE 5.** MSE of the advocated new hybrid ML-EM, the SISO DA LS in [1] (i.e.,  $N_r = 1$ ), and its proposed SIMO DA ML extension vs. the per-carrier SNR with QPSK,  $N_c = 3$ ,  $N_r = 2$ , and  $N_p = 8$  at: (a)  $v = 60$  km/h, and (b)  $v = 300$  km/h.

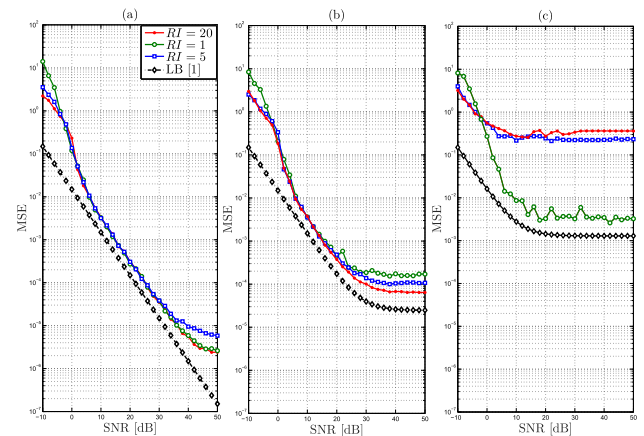


**FIGURE 6.** MSE of the advocated new hybrid ML-EM vs. the per-carrier SNR for different values of  $RI$  with QPSK,  $N_c = 3$ ,  $N_r = 2$ , and  $N_p = 8$  at: (a)  $v = 60$  km/h, (b)  $v = 300$  km/h, and (c)  $v = 600$  km/h.

This behavior stems from the fact that noise level at low and medium SNRs is much higher than the ICI component. Hence, the estimator performance is dictated by the noise level. At high per-carrier SNR, the ICI level becomes comparable to the noise level it follows that more ICIC iterations are required to provide better estimation accuracy.

In Fig. 6, we investigate the effect of the refreshment interval  $RI$  on the estimation accuracy of the proposed technique at low and high mobilities. At low Doppler (i.e., at velocity  $v = 60$  km/h), the hybrid ML-EM technique exhibits the same performance when initialized with DA ML at each OFDM block (i.e.,  $RI = 1$ ) or with less recurrent initialization (i.e.,  $RI = 20$ ). However, at high Doppler (i.e., at velocity  $v = 600$  km/h), we observe a significant deterioration when hybrid ML-EM is initialized at the rates of 5 or 20. This is hardly surprising because the channel varies slowly at low Doppler and the estimates provided during the previous  $N_c$  OFDM blocks become adequate initial guesses for the current  $N_c$  blocks. At high Doppler, however, the channel varies rapidly in time and the estimates of the previous blocks can no longer be considered as good candidates to trigger the estimation process during the following blocks.

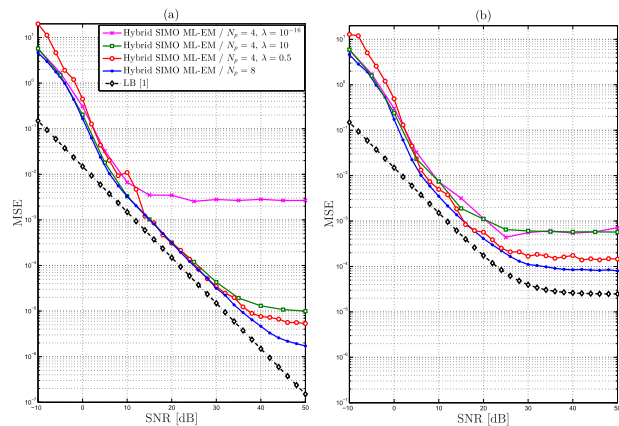


FIGURE 7. MSE of the advocated new hybrid ML-EM vs. the per-carrier SNR for different regularization factors of RDM at initialization with QPSK,  $N_r = 2$ , and  $N_c = 3$  at: (a)  $v = 60$  km/h, and (b)  $v = 300$  km/h.

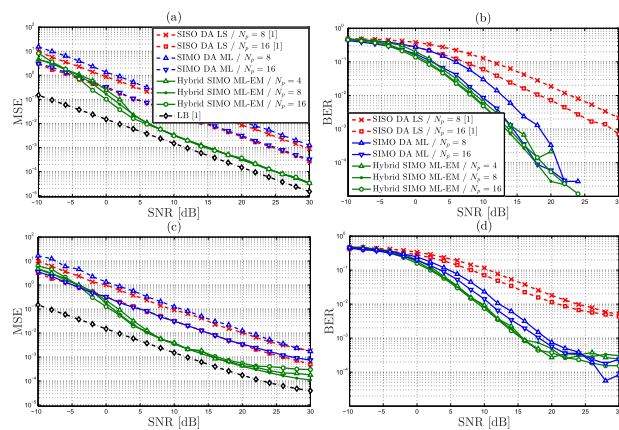


FIGURE 8. Performance of the advocated new hybrid ML-EM, the SISO DA LS in [1] (i.e.,  $N_r = 1$ ), and its proposed SIMO DA ML extension vs. the per-carrier SNR with QPSK,  $N_c = 3$  and  $N_r = 2$  in terms of: (a) MSE at  $v = 60$  km/h, (b) BER at  $v = 60$  km/h, (c) MSE at  $v = 300$  km/h, and (d) BER at  $v = 300$  km/h.

In Fig. 7, we investigate the impact of the regularization factor  $\lambda$  in initialization with SIMO RDM on the performance of the proposed hybrid ML-EM technique.

With an arbitrarily small regularization factor (i.e.,  $\lambda = 10^{-16}$ ), its performance deteriorates since its initialization with SIMO RDM suffers from the same instability issues of the SISO DA LS technique in [1] or its proposed SIMO DA ML extension. By increasing  $\lambda$ , its performance improves and approaches the estimation accuracy achieved with  $N_p = 8$  pilot tones. The latter corresponds to an overdetermined problem. However, for higher values of  $\lambda$ , the performance of hybrid ML-EM starts to deteriorate again since the SIMO RDM initialization solution departs significantly from the original one defined in (37) and becomes less sensitive to the received samples.

In Fig. 8, we assess the robustness of the proposed technique to the number of available per-carrier pilot frames. We see that the gap between the two techniques increases by reducing the number of pilots per OFDM block from  $N_p = 16$  to  $N_p = 8$ , more so at high Dopplers. Indeed,

both SISO DA LS in [1] and its proposed SIMO DA ML extension deteriorate in MSE performance by reducing  $N_p$  while the advocated hybrid ML-EM exhibits exactly the same performance at medium-to-high per-carrier SNR thresholds. Actually, hybrid ML-EM performs nearly the same in BER<sup>2</sup> as the proposed SIMO DA ML extension, yet with less pilots. Consequently, the new technique can achieve a higher per-carrier throughput by reducing the overhead by half. The number of pilots can even be further reduced to  $N_p = 4$  (up to 75% reduction), below the number of paths. In this configuration, both SISO DA LS in [1] and its proposed SIMO DA ML extension cannot provide reliable estimates. Whereas, the advocated hybrid ML-EM solution still works properly when initialized instead with SIMO RDM. As can be seen in Figs. 8 (a) and (c), the new technique exhibits approximately the same MSE performance, except for some negligible deterioration at high SNRs. Yet the latter does not affect the BER performance. Indeed, the proposed hybrid ML-EM performs nearly the same in BER regardless of the different numbers of pilots considered in Figs. 8 (b) and (d).

In Fig. 9, we plot the link-level per-carrier throughput curves of hybrid ML-EM. For a given modulation order  $M$ , please note that the per-carrier throughput can be obtained from the symbol error rate (SER) as follows:

$$\text{Throughput} = \frac{1}{T} \log_2(M)(1 - \text{SER})(1 - \Delta), \quad (41)$$

where  $\Delta$  is the overhead ratio computed as:

$$\Delta = \frac{N_p}{N R I}, \quad (42)$$

which becomes negligible at large values of  $RI$ . The latter cannot be, however, increased indefinitely as the hybrid ML-EM technique requires more frequent up-to-date initial estimates in the case of high mobility.

We see from Fig. 9 (a) that QPSK transmissions, among the considered modulations, provide higher per-carrier throughput at per-carrier SNR values below 4 dB. When the per-carrier SNR ranges between 4 and 14 dB, 16-QAM becomes more suitable whereas 64-QAM dominates when the per-carrier SNR exceeds 14 dB. The resulting per-carrier throughput curve assuming an adaptive (i.e., SNR-dependent) modulation is depicted by the black curve. In Fig. 9 (b), we show the performance of the hybrid ML-EM technique at a higher normalized Doppler  $F_D T = 0.1$ . In this scenario, QPSK, 16-QAM, and 64-QAM modulations provide higher per-carrier throughput over the same SNR ranges reported above at low Doppler. We also observe that both 16- and 64-QAM transmissions suffer from some performance degradation when compared to the low mobility scenario. Indeed,

<sup>2</sup>In the proposed SIMO DA ML extension and its SIMO RDM variant, we implement maximum ratio combining (MRC) over the  $N_r$  antenna branches prior to passing the resulting MRC output through an iterative SIC decoder as in SISO DA LS in [1]. Whereas we implement the MAP decoder in (30) with the advocated hybrid SIMO ML-EM solution or the proposed SIMO NDA ML version.

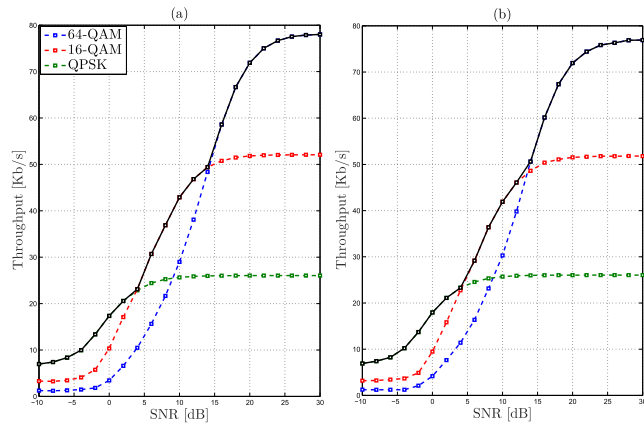


**FIGURE 9.** Link-level per-carrier throughput vs. the per-carrier SNR of the advocated new hybrid ML-EM with  $N_c = 3$ ,  $N_r = 2$ , and  $N_p = 8$  at: (a)  $v = 60$  km/h, and (b)  $v = 300$  km/h.

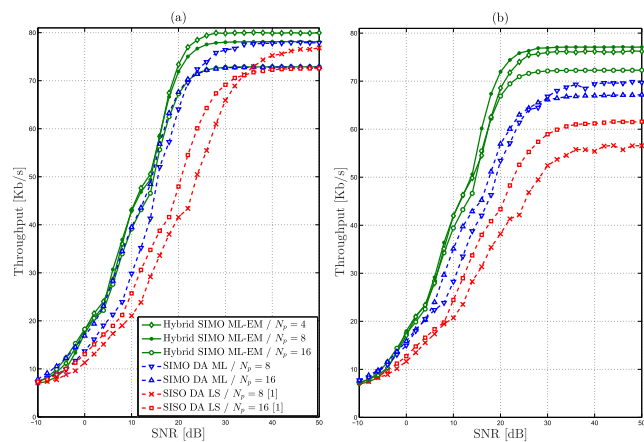


**FIGURE 10.** Link-level per-carrier throughput vs. the per-carrier SNR of the advocated new hybrid ML-EM, the SISO DA LS in [1] (i.e.,  $N_r = 1$ ), and its proposed SIMO DA ML extension with  $N_c = 3$ ,  $N_r = 2$ , and  $\lambda = 0.5$  at: (a)  $v = 60$  km/h, and (b)  $v = 300$  km/h.

at lower Doppler values, the hybrid technique provides accurate estimates since the channel varies slowly during the same period. Hence, the decoder at the destination is able to accurately decode the transmitted symbols. In the case of high mobility, the channel varies rapidly during the same period, leading to a more severe degradation of the channel estimates. The latter affects the decoding process, especially at higher-order modulations which are more sensitive to phase shifts.

In Fig. 10, we plot the link-level per-carrier throughput curves of the hybrid ML-EM, the SISO DA in [1], and the proposed SIMO DA ML extension assuming an adaptive (i.e., SNR-dependent) modulation scheme. Here, we report a clear advantage in throughput performance of the hybrid ML-EM technique, especially at higher mobility (i.e.,  $F_D T = 0.1$ ) and modulation orders (i.e., 16- and 64-QAM). As reported previously, the SISO DA LS technique in [1] and its proposed SIMO DA ML extension provide less reliable channel estimates since both operate only at pilot symbols. These estimates lead to higher BER when injected later at the data

samples in the MRC-SIC decoding process. Moreover, from Fig. 10 (b), we observe that the performance of both SISO DA in [1] and its proposed SIMO DA ML extension significantly deteriorates when the number of pilots reduces by half from 16 to 8. Such losses stem from the fact that poor channel gain estimates result in less reliable ICIC, especially at higher modulation orders. Even though the proposed SIMO DA ML extension takes advantage of antenna diversity, it still exhibits the same behaviour as the SISO DA LS original version in [1] since the quality of channel estimates also deteriorates when the number of pilots decreases. On the other hand, the advocated hybrid ML-EM maintains approximately the same performance in terms of MSE whether initialized with  $N_p = 4$ , 8 or 16 Per-carrier pilot frame. Hence, it exhibits higher link-level per-carrier throughputs, more so at medium or high per-carrier SNR levels, with best performance achieved when  $N_p = 4$  pilots.

In Fig. 11, we plot the link-level per-carrier throughput curves of the advocated hybrid ML-EM - when operated at multiple refreshment rates - and both SISO DA LS in [1] and its proposed SIMO DA ML extension to assess more thoroughly their robustness to mobility. We see from Figs. 11 (a) and (b) that the per-carrier throughput increases with hybrid ML-EM at low to medium Doppler once the refreshment interval  $RI$  jumps from 1 to 5. This is hardly surprising since the channel varies slowly in time and, hence, the channel coefficients of the previous OFDM blocks act as extremely reliable initial guesses for the current OFDM blocks. It follows that the pilot subcarriers are no longer required at the current OFDM blocks and can be used to carry data instead. Pilot insertion rate can be slowed down significantly, by at least as much as 20 times (pilot to data or overhead ratio can become as low as 0.16%), while still reporting some noticeable throughput gains instead of losses, more so at high per-carrier SNR! Whereas SISO DA LS in [1] and its proposed SIMO DA ML extension still require the same amount of pilots to provide reliable channel estimates. Therefore, no additional throughput gains can be achieved. At high Doppler, however, the channel varies more rapidly and more frequent initialization is needed. As can be observed in Fig. 11 (c), we start to measure increasingly significant per-carrier throughput losses as the refreshment interval  $RI$  increases. Yet, most importantly, our new hybrid ML-EM technique still outperforms both SISO DA LS in [1] and its proposed SIMO DA ML extension in all considered scenarios, more so over increasingly faster time-varying channels. Here, we have to reduce  $RI$  at least from 20 to 5 among three tested values, or ultimately to 1 in order to secure the highest reported gains in throughput achievable among the three  $RI$ -dependent scenarios. Actually, one can reach the maximum achievable throughput performance after offline optimization<sup>3</sup> of the refreshment interval  $RI$  against mobility.

<sup>3</sup>To obtain the optimal value of  $RI$ , the performance of the new hybrid ML-EM can be evaluated offline in different scenarios over multiple combinations of the average per-carrier SNR, Doppler, and  $RI$  values. However, this ad hoc offline optimization step is beyond the scope of this work.

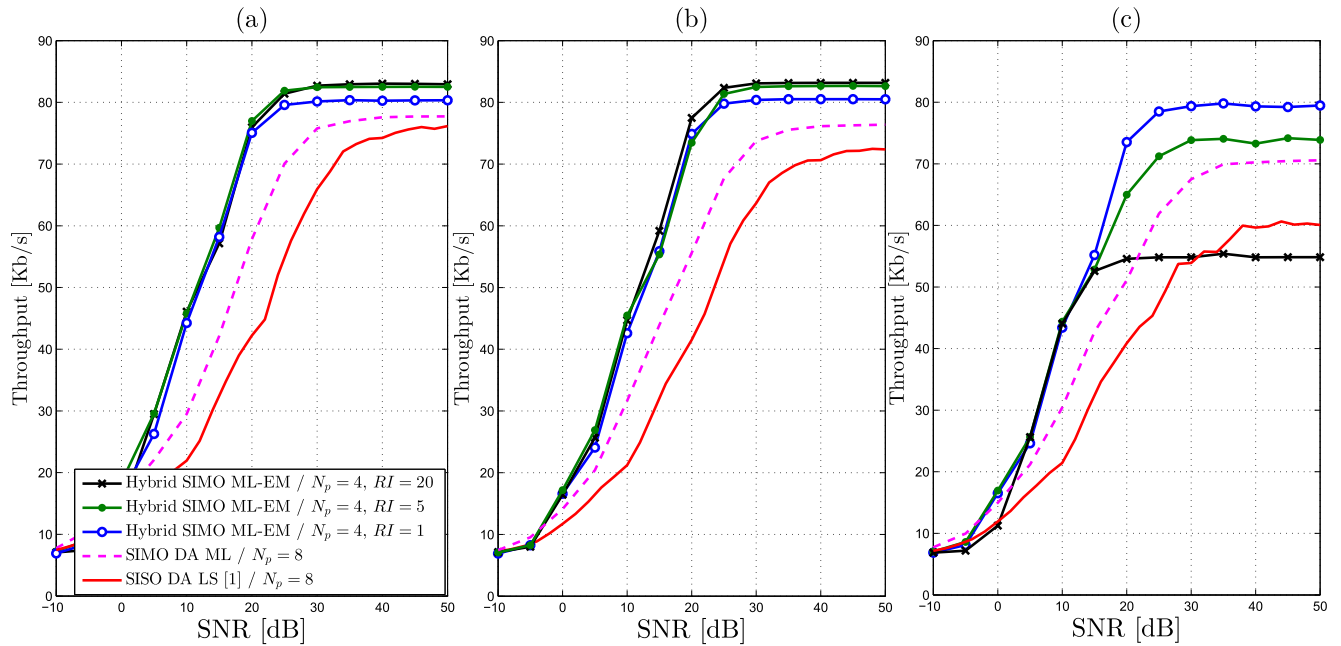


**FIGURE 11.** Link-level per-carrier throughput vs. the per-carrier SNR of the advocated new hybrid ML-EM (with  $N_p = 4$ ) at multiple  $RI$  values, the SISO DA LS in [1] (i.e.,  $N_r = 1$ ), and its proposed SIMO DA ML extension (with  $N_p = 8$ ) with  $N_c = 3$ ,  $N_r = 2$ , and  $\lambda = 0.5$  at: (a)  $v = 60$  km/h, (b)  $v = 120$  km/h, and (c)  $v = 240$  km/h.

**VI. CONCLUSION**

In this paper, we addressed the problem of time-varying channel estimation over SIMO OFDM transmissions in multipath propagation environments. The proposed approach is based on a polynomial approximation of the complex path gains and takes advantage of all the observation - both at pilot and non-pilot positions - to enhance the channel estimation capabilities. To do so, we develop a new SIMO DA ML estimator - which turns out to be a generalized extension of the SISO DA LS estimator in [1] - for the sole purpose of initializing at relatively rare pilot insertion instants (pilot to data or overhead ratio can be as low as 0.16%) of another new SIMO NDA ML version when operated at the remaining data samples, resulting in the ultimately advocated new hybrid ML-EM estimator of fast time-varying OFDM channels. Moreover, by further developing a new regularized DA ML (RDM) variant of either SISO DA LS in [1] or its proposed SIMO DA ML extension, we were able to further reduce the number of pilots and break the strict requirement of more pilots than paths in [1], and, hence, decrease the overhead and increase the per-carrier throughput. We show through exhaustive simulations that the proposed hybrid ML-EM solution outperforms both SISO DA LS in [1] and its proposed SIMO DA ML extension in terms of component-level channel identification accuracy. The latter translates into significant gains in terms of link-level BER and per-carrier throughput performances, especially at medium-to-high per-carrier SNR values more so at relatively higher Doppler or faster SIMO OFDM channel variations.

**REFERENCES**

[1] H. Hijazi and L. Ros, "Polynomial estimation of time-varying multipath gains with intercarrier interference mitigation in OFDM systems," *IEEE Trans. Veh. Technol.*, vol. 58, no. 1, pp. 140–151, Jan. 2009.

[2] NR; *Physical Channels and Modulation*, document G.T.38.211, 2018.

[3] P. Banelli, S. Buzzi, G. Colavolpe, A. Modenini, F. Rusek, and A. Ugolini, "Modulation formats and waveforms for 5G networks: Who will be the heir of OFDM?: An overview of alternative modulation schemes for improved spectral efficiency," *IEEE Signal Process. Mag.*, vol. 31, no. 6, pp. 80–93, Nov. 2014.

[4] S. Affes and P. Mermelstein, "Adaptive space-time processing for wireless CDMA," in *Adaptive Signal Processing: Application to Real-World Problems*, vol. 10, J. Benesty and A. H. Huang, Eds. Berlin, Germany: Springer, 2003, pp. 283–321.

[5] I. Mrissa, F. Bellili, S. Affes, and A. Stéphenne, "A context-aware cognitive SIMO transceiver for enhanced throughput on the downlink of LTE HetNet," *Wireless Commun. Mobile Comput.*, vol. 16, no. 11, pp. 1414–1430, Aug. 2016.

[6] I. Mrissa, F. Bellili, S. Affes, and A. Stéphenne, "A cognitive MIMO transceiver for enhanced 4G and beyond link-level throughput," in *Proc. IEEE PIMRC*, Montreal, QC, Canada, Oct. 2017, pp. 1–5.

[7] M. A. Boujelben, F. Bellili, S. Affes, and A. Stéphenne, "SNR estimation over SIMO channels from linearly modulated signals," *IEEE Trans. Signal Process.*, vol. 58, no. 12, pp. 6017–6028, Dec. 2010.

[8] Z. Tang, R. C. Cannizzaro, G. Leus, and P. Banelli, "Pilot-assisted time-varying channel estimation for OFDM systems," *IEEE Trans. Signal Process.*, vol. 55, no. 5, pp. 2226–2238, May 2007.

[9] S. Tomasin, A. Gorokhov, H. Yang, and J. P. Linnartz, "Iterative interference cancellation and channel estimation for mobile OFDM," *IEEE Trans. Wireless Commun.*, vol. 4, no. 1, pp. 238–245, Jan. 2005.

[10] Y. Mostofi and D. C. Cox, "ICI mitigation for pilot-aided OFDM mobile systems," *IEEE Trans. Wireless Commun.*, vol. 4, no. 2, pp. 765–774, Mar. 2005.

[11] H. Senol, E. Panayirci, and H. V. Poor, "Nondata-aided joint channel estimation and equalization for OFDM systems in very rapidly varying mobile channels," *IEEE Trans. Signal Process.*, vol. 60, no. 8, pp. 4236–4253, Aug. 2012.

[12] S. B. Amor, S. Affes, and F. Bellili, "ML EM estimation of fast time-varying OFDM-type channels," in *Proc. IEEE IWCMC*, Tangier, Morocco, Jun. 2019, pp. 1–6.

[13] A. Wiesel, J. Goldberg, and H. Messer-Yaron, "SNR estimation in time-varying fading channels," *IEEE Trans. Commun.*, vol. 54, no. 5, pp. 841–848, May 2006.

[14] F. Bellili, R. Meftehi, S. Affes, and A. Stéphenne, "Maximum likelihood SNR estimation of linearly-modulated signals over time-varying flat-fading SIMO channels," *IEEE Trans. Signal Process.*, vol. 63, no. 2, pp. 441–456, Jan. 2015.

- [15] F. Bellili, A. Stéphanne, and S. Affes, "SNR estimation of QAM-modulated transmissions over time-varying SIMO channels," in *Proc. IEEE Int. Symp. Wireless Commun. Syst.*, Reykjavik, Iceland, Oct. 2008, pp. 199–203.
- [16] H. Hijazi and L. Ros, "Joint data QR-detection and Kalman estimation for OFDM time-varying Rayleigh channel complex gains," *IEEE Trans. Commun.*, vol. 58, no. 1, pp. 170–178, Jan. 2010.
- [17] H. Hijazi, P. E. Simon, M. Liénard, and L. Ros, "Channel estimation for MIMO-OFDM systems in fast time-varying environments," in *Proc. 4th Int. Symp. Commun., Control Signal Process. (ISCCSP)*, Limassol, Cyprus, Mar. 2010, pp. 1–6.
- [18] R. Yang, S. Ye, P. Si, Y. Teng, and Z. Yanhua, "Iterative channel estimation and detection for high-mobility MIMO-OFDM systems: Mitigating error propagation by exploiting error information," *Wireless Pers. Commun.*, vol. 84, no. 3, pp. 1907–1931, Oct. 2015.
- [19] A. P. Dempster, N. M. Laird, and D. B. Rubin, "Maximum likelihood from incomplete data via the EM algorithm," *J. Roy. Statist. Soc., B (Methodol.)*, vol. 39, no. 1, pp. 1–38, 1977.
- [20] F. Bellili, A. Methenni, S. B. Amor, S. Affes, and A. Stéphanne, "Time synchronization of turbo-coded square-QAM-modulated transmissions: Code-aided ML estimator and closed-form Cramér–Rao lower bounds," *IEEE Trans. Veh. Technol.*, vol. 66, no. 12, pp. 10776–10792, Dec. 2017.
- [21] G. Golub, P. C. Hansen, and D. O'Leary, "Tikhonov regularization and total least squares," *SIM J. Matrix Anal. Appl.*, vol. 21, no. 1, pp. 185–194, 1999.
- [22] F. Wang, S. Chawla, and W. Liu, "Tikhonov or lasso regularization: Which is better and when," in *Proc. IEEE 25th Int. Conf. Tools Artif. Intell.*, Herndon, VA, USA, Nov. 2013, pp. 795–802.



**SOUHEIB BEN AMOR** was born in Hammam sousse, Sousse, Tunisia, in 1989. He received the Diplôme d'Ingénieur in telecommunications from the National Engineering School of Tunis, in 2013, and the M.Sc. degree from the Institut National de la Recherche Scientifique-Énergie, Matériaux, et Télécommunications (INRS-ÉMT), Université du Québec, Montréal, QC, Canada, in 2016, where he is currently pursuing the Ph.D. degree. He held an internship with Ericsson Canada, in winter 2015, as a part of the Create-Perswade Training Program. He was also a Research Intern with Interdigital Canada, in summer 2015. His Ph.D. program is in the field of statistical signal processing and array processing and their applications in wireless communications. He received a scholarship for M.Sc. studies under the agreement between the Tunisian Government and INRS-ÉMT. He also received the INRS scholarship for his Ph.D. studies.



**SOFIÉNE AFFES** (S'94–M'95–SM'05) received the Diplôme d'Ingénieur degree in telecommunications and the Ph.D. degree (Hons.) in signal processing from Télécom ParisTech (ENST), Paris, France, in 1992 and 1995, respectively. He was a Research Associate with INRS, Montreal, QC, Canada, until 1997, an Assistant Professor, until 2000, and an Associate Professor, until 2009. He is currently a Full Professor and the Director of PERWADE, a unique M4 million research-training program on wireless in Canada involving 27 partners from eight universities and ten industrial organizations. He has been twice a recipient of the Discovery Accelerator Supplement Award from NSERC, from 2008 to 2011 and from 2013 to 2016. From 2003 to 2013, he was the Canada Research Chair in wireless communications. Since October 2017, he holds a Cyrille-Duquet Research Chair in telecommunications. In 2006, 2015, and 2017, he served as the General Co-Chair or Chair of the IEEE VTC'2006-Fall, the IEEE ICUWB'2015, the IEEE PIMRC'2017, and co-located the IEEE 5G Summit, respectively, all held in Montreal, QC, Canada. In 2008 and 2015, he received

the IEEE VTC Chair Recognition Award from the IEEE VTS and the IEEE ICUWB Chair Recognition Certificate from the IEEE MTT-S for exemplary contributions to the success of both events, respectively. He has previously served as an Associate Editor for the IEEE TRANSACTIONS ON WIRELESS COMMUNICATIONS, the IEEE TRANSACTIONS ON COMMUNICATIONS, the IEEE TRANSACTIONS ON SIGNAL PROCESSING, the *Hindawi Journal of Electrical and Computer Engineering*, and the *Wiley Journal of Wireless Communications and Mobile Computing*. He currently serves as a member of the Editorial Board of the *MDPI Sensors Journal* and the Advisory Board of the *MDPI Multidisciplinary Journal Sci*. He has been a member of the Canadian Evaluation Group (CEG) and the Canadian National Organization (CNO), since 2009 and 2017, respectively, involved from Canada in the Working Party 5D (WP 5D) activities for the ITU on IMT-Advanced and IMT-2020.



**FAOUZI BELLILI** received the B.Eng. degree (Hons.) in electrical engineering from Tunisia Polytechnic School, in 2007, and the M.Sc. (Hons.) and Ph.D. (Hons.) degrees from the National Institute of Scientific Research (INRS), University of Quebec, Montreal, QC, Canada, in 2009 and 2014, respectively. From September 2014 to September 2016, he was working as a Research Associate with INRS-EMT, where he coordinated a major multiinstitutional NSERC Collaborative R&D (CRD) Project on 5th-Generation (5G) Wireless Access Virtualization Enabling Schemes (5G-WAVES). From December 2016 to May 2018, he was a Postdoctoral Fellow with the University of Toronto, ON, Canada. He is currently an Assistant Professor with the Department of Electrical and Computer Engineering, University of Manitoba, Winnipeg, MB, Canada. His researches focus on statistical and array signal processing for wireless communications and 5G-enabling technologies. He was awarded the very prestigious NSERC PDF Grant over the period 2017–2018. He was also awarded another prestigious PDF Scholarship offered over the same period (but declined) from the "Fonds de Recherche du Québec Nature et Technologies" (FRQNT). He was also awarded the INRS Innovation Award for the year 2014/2015, the very prestigious Academic Gold Medal of the Governor-General of Canada for the year 2009–2010, and the Excellence Grant of the Director-General of INRS for the year 2009–2010. He received the Award of the best M.Sc. Thesis in INRS-EMT for the year 2009–2010 and twice - for both the M.Sc. and Ph.D. programs - the National Grant of Excellence from the Tunisian Government. In 2011, he was also awarded the Merit Scholarship for Foreign Students from the Ministère de l'Éducation, du Loisir et du Sport (MELS) of Quebec, Canada. He serves regularly as a TPC member for major IEEE conferences and acts as a Reviewer for many international scientific journals and conferences.



**DUSH NALIN JAYAKODY** (M'14–SM'18) received the B.Eng. degree (Hons.) from Pakistan and was ranked as the merit position holder of the University (under SAARC Scholarship), the M.Sc. degree in electronics and communications engineering from Eastern Mediterranean University, Cyprus (under the University full graduate scholarship) and ranked as the first merit position holder of the department, and the Ph.D. degree in electronics and communications engineering from the University College Dublin, Ireland. From 2014 to 2016, he held a postdoctoral position with the University of Tartu, Estonia, and the University of Bergen, Norway. Since 2016, he has been an Associate Professor with the Institute of Cybernetics, National Research Tomsk Polytechnic University, Russia, where he also serves as the Director of the Tomsk Infocomm Laboratory.

• • •